Implications of observation error correlation on the assimilation of interferometric radiances

Reima Eresmaa, Niels Bormann and Anthony P. McNally

European Centre for Medium-range Weather Forecasts
Reading, Berkshire, United Kingdom

1 Introduction

Current practice is to dissiminate and assimilate infrared interferometer radiances in apodized form such that undesired side-lobe effects, that are introduced during transitioning from measured interferogram to observed radiance, are minimized. Use of apodized radiances simplifies forward modelling by localizing channel response functions, but there is a drawback that effective spectral resolution is degraded. Additionally, observation error correlations (OEC) are introduced between channels that are located near to each other in the spectrum.

The most important infrared interferometers in current numerical weather prediction (NWP) applications include the Infrared Atmospheric Sounding Interferometer (IASI), onboard the Metop A/B satellites, and the Cross-track Infrared Sounder (CrIS), onboard the Suomi-NPP polar orbiter. At the European Centre for Medium-range Weather Forecasts (ECMWF), radiance data from IASI have been used in the operational system since 2007, while CrIS radiances have not yet entered the operational suite.

Initially justified by computational simplicity and lack of good knowledge of OEC, the operational radiance assimilation at ECMWF assumes uncorrelated observation errors. The assumption is reflected in the assimilated IASI channel subset. Only a few pairs of spectrally-adjacent channels are assimilated so that the effect of the signal apodization can safely be ignored. The assimilated channel subset originates from the 300-channel list proposed by Collard (2007), although channels have since been added in order to strengthen the temperature analysis in the tropopause region (Collard and McNally, 2009). Today, 373 IASI channels are operationally monitored, and up to 191 channels (depending on cloud conditions) are allowed to have a significant weight in the data assimilation. The choice of assimilated channels puts emphasis on efficient use of long-wave channels that are sensitive to carbon dioxide only.

Recently, Ventress and Dudhia (2014) demonstrated that theoretically-derived channel selections are sensitive to assumptions made with regard to OEC. Furthermore, they proposed a methodological extension that aims at optimizing the radiance assimilation in the presence of OEC, provided that the data assimilation sticks to the use of a diagonal observation error covariance matrix.

Since the early work on the use of IASI radiances, empirical studies have increased our knowledge on OEC (Bormann et al., 2009). Furthermore, computational feasibility of explicit treatment for inter-channel OEC in realistic NWP applications has been demonstrated (Weston et al., 2014). The radiance assimilation using a full (non-diagonal) observation error covariance matrix is currently being tested at ECMWF.

Combining the two parallel lines of development, the work presented in this paper is motivated with the aim at optimizing the assimilated channel subset in the presence of OEC with the intention to explicitly account for the OEC in the data assimilation. We restrict ourselves to accounting for the OEC introduced through the signal apodization, as these error correlations are fully known from theoretical considerations. The paper is structured as follows. We will first demonstrate the effect of OEC on information content in an extremely simple and hypothetical linear analysis system (Section 2). This is followed by brief discussion on known characteristics of OEC in the special case of IASI radiances in Section 3. We devote Section 4 to investigating the effect that OEC has on theoretically-optimized channel selections. As an outcome from this, we derive two new channel lists which are evaluated in theoretical and practical means in Section 5. Section 6 summarizes the results.

2 Theoretical effect of OEC on observation information content

Let us consider information content of observations in a hypothetical two-parameter analysis system, where each parameter is directly observed by one (and only one) observation. Moreover, let us set observation and background error variances to unity and assume that observation and background errors do not correlate with each other (but allow correlated observation errors and correlated background errors). We quantify the observation information content using a theoretical concept of the Degrees of Freedom for the Signal (DFS), defined as

$$\mathrm{DFS} \quad = \quad tr\left(\mathbf{I} - \mathbf{A}\mathbf{B}^{-1}\right), \tag{1}$$

where $\mathbf{A}$ and $\mathbf{B}$ are analysis and background error covariance matrices, respectively, and $\mathbf{I}$ is an identity matrix. Assuming an optimal analysis system, $\mathbf{A}$ depends on observation operator $\mathbf{H}$, gain matrix $\mathbf{K}$ and $\mathbf{B}$ through

$$\mathbf{A} \quad = \quad (\mathbf{I} - \mathbf{K}\mathbf{H})\,\mathbf{B}, \tag{2}$$

whereas observation error covariance matrix $\mathbf{R}$ plays a role in determining $\mathbf{K}$ through

$$\mathbf{K} \quad = \quad \mathbf{B}\mathbf{H}^T\left(\mathbf{H}\mathbf{B}\mathbf{H}^T + \mathbf{R}\right)^{-1}. \tag{3}$$

Note that in this hypothetical system $\mathbf{H}$=$\mathbf{I}$.

In the hypothetical analysis system, the DFS depends only on correlations specified for the observation error and the background error. This dependence is shown in Fig. 1. In the case that neither observation errors nor background errors correlate (i.e., in the middle of the plot), the DFS equals 1. Introducing (either positive or negative) background error correlation decreases the DFS, while the effect of introducing (either positive of negative) OEC is to increase the DFS. The interpretation is that the observations are the most beneficial to the analysis when either little is known about the background parameters (i.e., background errors are uncorrelated) or much is known about observations (i.e., observation errors are correlated). It is worth noting that the graph in Fig. 1 is not exactly symmetrical around its axes: in the case where the background error is almost fully correlated, introducing positive OEC has a detrimental impact on the DFS.

Given that the two analysis variables here are directly observed by two observations, the system described above represents any analysis that is based on two observations and computed in observation

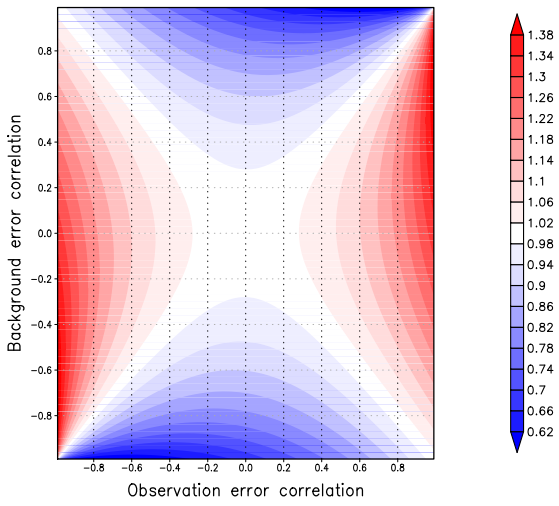

Fig. 1: Degrees of Freedom for the Signal (DFS) as a function of observation and background error correlations in a hypothetical two-parameter analysis system.

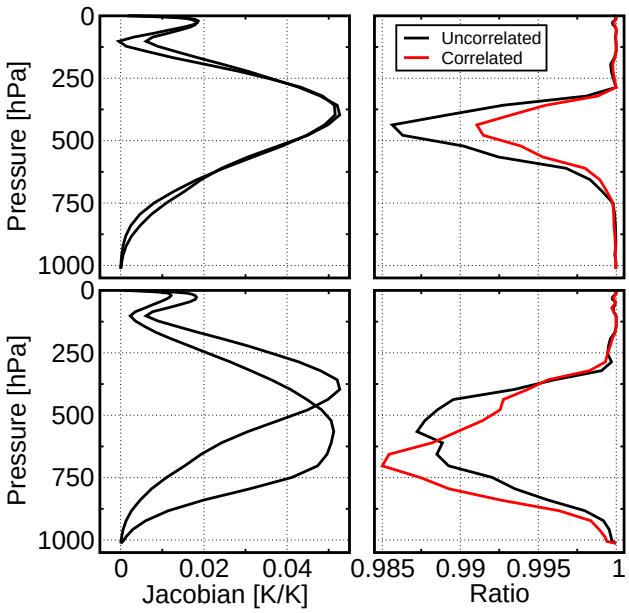

Fig. 2: Ratio of analysis and background error standard deviations in one-dimensional temperature analysis based on two IASI channels (right panels). Jacobians of the used channels are shown in the left panels.

space. In this framework, background error correlation relates to similarity of the two observations. This is illustrated in Fig. 2 for temperature analysis using two IASI channels. Two scenarios are considered. In the first scenario (upper panels), the two channels are sensitive to same atmospheric layers. Referring to Fig. 1, this corresponds to a situation where background error correlation ≈ 1, and the analysis does not benefit from the presence of OEC. Instead, introducing OEC increases the analysis error standard deviation considerably. In the second scenario (bottom panels), the two channels peak at different altitudes and the amount of overlap in their Jacobians is considerably reduced. This corresponds to a situation where background error correlation is smaller than 1, and we find introduction of OEC to result in improved analysis accuracy in the lower troposphere. We conclude that presence of OEC is really beneficial to the analysis accuracy only when the two channels are sensitive to different things, i.e., when their Jacobians overlap only partially.

3 Characteristics of OEC in the special case of infrared interferometers

Diagnostic studies such as those in Bormann et al. (2009) and Weston et al. (2014) suggest correlations of varying strength throughout the spectrum observed by infrared sounders. In particular, channels in the main water vapour absorption band are typically found to share OEC, and strong OEC are diagnosed also between window channels. The origin of these OEC is not fully understood (although contributions from forward modelling and representativeness are commonly suspected) and there is some uncertainty surrounding the values of the estimated correlations due to assumptions made in the diagnostic tools.

However, the inter-channel OEC introduced by the signal apodization is well known. Using the signal processing theory and knowing characteristics of the applied apodization function, the OEC associated to the signal apodization can be quantified accurately. In the case of IASI, the associated OEC is 0.70 (0.25) between any pair of spectrally-adjacent (spectrally-alternate) channels.

4 Effect of OEC on the optimization of channel selection

Using a highly-simplified linear analysis framework, it was shown in Section 2 that presence of OEC can have a beneficial impact on observation information content, but this requires that observations sharing

the OEC measure sufficiently different quantities. Implications from this result in a realistic NWP framework are not obvious, as number of assimilated channels can be in the order of hundreds, observations represent broad vertical integrals of temperature and humidity, and background error characteristics are complicated. Given that error correlations related to representativeness issues or forward modelling are arguably the strongest in those channel pairs that are the most similar in their sensitivities to atmospheric variables, one would perhaps not expect much increase in the information content even if the OEC was accounted for in the channel selection. On the other hand, the OEC related to the signal apodization can potentially be exploited in the channel selection, given that pairs of neighbouring channels with non-overlapping Jacobians are identified.

With these considerations in mind, we have derived an alternative OEC-based channel list for the assimilation of IASI radiances such that the OEC introduced by the signal apodization is explicitly taken into account. In order to study the effect that the OEC has on channel selection in particular, we have additionally derived a reference channel list that assumes no OEC to be present in the data. Without the reference list the OEC-based list could only be compared with the operational list, and it would be difficult to tell which differences are due to the OEC. The operationally-used channel list reflects choices made in response to practical issues that are too complicated to be handled in theoretical computations.

The two channel lists are produced using the following procedure:

1. Use the operational list of actively-assimilated 191 channels as a starting point.
2. Find the least useful channel included in the current list by removing one channel at a time and re-computing the DFS.
3. Remove the least useful channel from the list.
4. Find the most useful channel not yet included in the current list by adding one channel at a time and re-computing the DFS.
5. Add the most useful channel to the list.
6. If the channel added in step 5 is the same as the one removed in step 3, exit the algorithm. Otherwise go back to step 2.

The algorithm maximizes the overall DFS of the selection while keeping the number of channels unchanged and it is run separately for the OEC-based and reference lists. Between the two runs, rules of computing the DFS are changed such that the full non-diagonal observation error covariance matrix is applied only while producing the OEC-based list[1]. Production of the reference list is based on a diagonal matrix, i.e., uncorrelated observation errors are assumed. Additionally, the pool of channels available to be selected is artificially restricted in the reference case so that channels adjacent to those already included in the list are not allowed to be chosen. The latter restriction is added in order to maintain similarity with the selection procedure of Collard (2007).

As we are mostly interested in temperature sounding channels in the long-wave CO_2 absorption band, changes made to the channel lists are restricted to first 600 IASI channels (spanning the wavenumber range of 645–794.75 cm^{-1}). We specify observation error standard deviations using a 4th-order polynomial fit shown in the top panel of Fig. 3; the fit is based on standard deviation of observed minus background departure on operationally-assimilated IASI channels, as determined from an earlier assimilation experiment. The background error covariance matrix is specified consistently with that used in the Integrated Forecasting System (IFS) at ECMWF, although it is modified for 1D-Var applications. Observation operator is constructed from temperature, humidity, ozone mixing ratio, and skin temperature Jacobians, that are determined using an offline version of RTTOV 9.3 and assuming two reference profiles that correspond to mid-latitude summer and winter conditions. The DFS is computed from the full analysis state vector consisting of skin temperature and profiles of temperature, humidity and ozone mixing ratio.

[1]It is still assumed that the signal apodization is the only source of OEC.

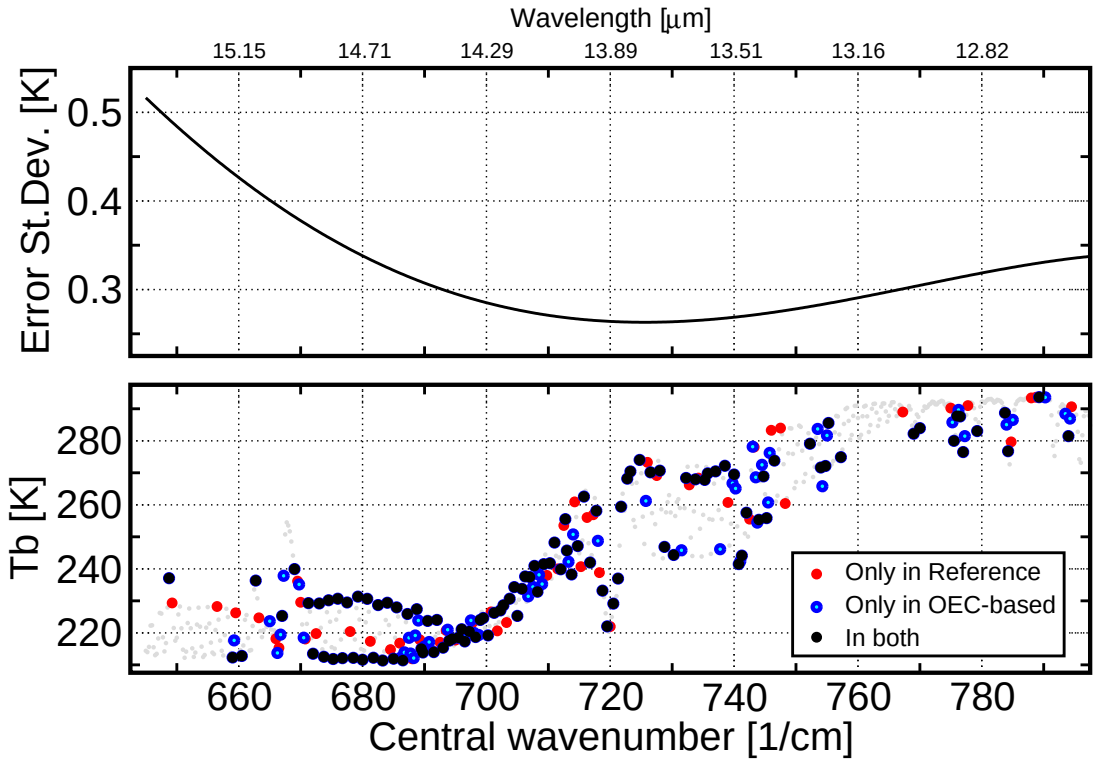

Fig. 3: Top: Observation error standard deviation specified to IASI channels during the production of the new channel lists. Bottom: Simulated long-wave IASI brightness temperature spectrum highlighting channels included in the reference (red dots), OEC-based (blue circles) and both (black dots) channel lists.

The output OEC-based and reference channel lists are compared in the bottom panel of Fig. 3. The grey dots represent a simulated brightness temperature spectrum corresponding to cloud-free conditions in a tropical reference atmosphere, while channels included in the reference list, OEC-based list, and both lists are indicated by red dots, blue circles, and black dots, respectively. Broadly speaking, the reference list contains more stratospheric- and upper-tropospheric-sensitive channels in the wavenumber range 645–720 cm^{-1}, whereas the OEC-based list contains more lower-tropospheric-sensitive channels between 720–800 cm^{-1}. It is noteworthy that those lower-tropospheric channels that are included only in the OEC-based list hit water vapour absorption lines. It appears that when the OEC is taken into account in the channel selection, smaller number of channels is required for constraining temperature analysis in the lower stratosphere and upper troposphere, allowing the use of more channels in constraining lower-tropospheric temperature and humidity analysis.

5 Performance evaluation

5.1 Theoretical information content

The two channel lists are compared in theoretical sense in Table 1 and Fig. 4. Table 1 shows DFS values at the start and end of the optimization process separately for the reference and OEC-based channel lists. Note that although the process is in both cases started from the operational list, the DFS values at the start differ from each other. This is because the computation of DFS makes use of the full non-diagonal observation error covariance matrix only when the OEC-based list is being produced. As compared with the reference case, the optimization process for the OEC-based list contains twice as many iterations and ends in higher DFS value, despite the DFS at the start being lower. This is most obvious from the normalized DFS values shown on the lowest row of the table (normalization is with respect to maximum

Table 1: Evolution of the DFS during the production of the reference and OEC-based channel lists.

	Reference	OEC-based
Iterations	38	76
DFS (start)	11.02	10.73
DFS (end)	11.84	12.14
% of max. available	76.7	83.7

available DFS that would be obtained if all of the first 600 channels were included in the selection).

Figure 4 shows profiles of DFS contribution (i.e., referring to Eq. (1), diagonal elements of $\mathbf{I}\text{-}\mathbf{AB}^{-1}$) in temperature (left panels) and humidity (right panels) analysis for the OEC-based (blue), reference (red), and operational (green) channel lists. The DFS contributions are shown both for the assumption of uncorrelated observation errors (top panels) and for the assumption that OEC is only due to the signal apodization (bottom panels). In all cases, the DFS contribution peaks around 400–500 hPa and is relatively large in a thick layer extending from 350 to 850 hPa. This is the layer where the applied channel selections provide the largest uncertainty reduction. Regardless of whether OEC is or is not taken into account, the new channel lists outperform the operational channel list, especially in the tropospheric humidity analysis. This happens because practical difficulties limit the number of humidity-sensitive channels in the operational list, whereas the new channel lists are optimized by theoretical means only. When the OEC is taken into account, the OEC-based list outperforms the reference list in the analysis of upper- and lower-tropospheric humidity and mid-tropospheric temperature. The performance gain can almost entirely be attributed to the effect of OEC (and not so much to the larger pool of channels

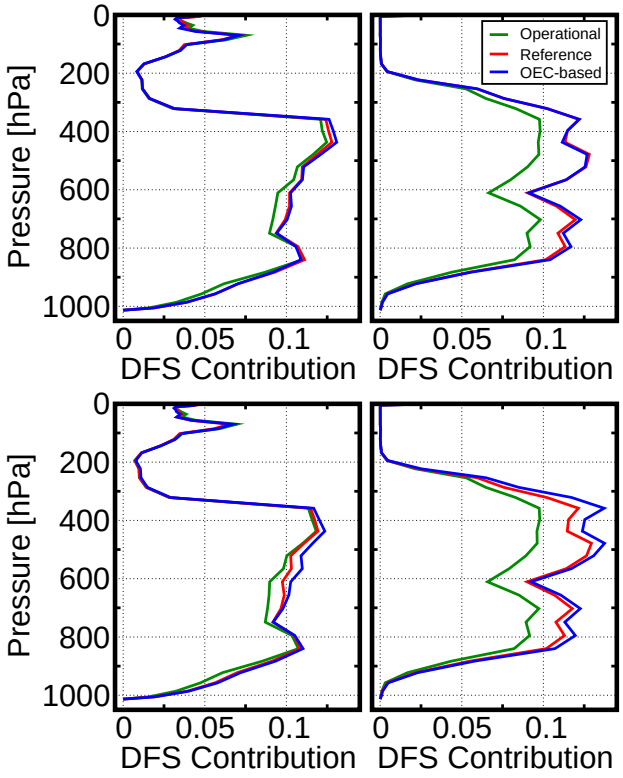

Fig. 4: Theoretical DFS contributions in temperature (left) and humidity (right) analysis in operational (green), reference (red) and OEC-based (blue) channel lists. Top (bottom) panels are for the assumption of uncorrelated (correlated) observation errors.

available for selection), as there is only little difference in performance when the DFS contributions are computed assuming uncorrelated observation errors. In the latter case, the slight performance gain in lower-tropospheric humidity analysis is caused by differences in sensitivity to water vapour absorption.

5.2 Practical performance

The new channel lists are next evaluated in terms of practical performance in a realistic NWP system. Three experiment runs are carried out using the global NWP system of ECMWF. The runs are based on model version Cy38r2 (that was operational from June to November 2013) using horizontal resolution T511 and 91 model levels in vertical. Apart from the IASI radiances, usage of observations is kept similar to the operational system. The runs cover the 90-day time period from 24 July to 21 October 2012, but the first week of each run is removed from the evaluation because of possible spin-up effects caused by lack of realistic initial bias correction coefficients.

Each run assimilates 191 IASI channels. In the first run ("operational run"), the operationally-used list of channels is assimilated. The second ("reference run") and third ("OEC-based run") runs, respectively, assimilate the reference and OEC-based channel lists. In all runs, the setup for the cloud detection and variational bias correction is unchanged from operational setting, as is the specification of observation error standard deviations. The operational and reference runs apply a diagonal observation error covariance matrix, whereas OEC is explicitly taken into account in the OEC-based run. The signal apodization is still assumed to be the only source of OEC, though.

Analysis fit to actively-assimilated IASI window and water-vapour channels is inter-compared between the three runs in Fig. 5. The indicated channels are the same in all runs (as they are not affected by the channel list optimization process). The statistics are shown separately for the extratropics and tropics. In all verification domains, both the reference and OEC-based run show improved analysis fit on low-peaking water-vapour channels (channel indices 2889–2958 and 5381–5480), although these channels show little difference between the reference and OEC-based runs. On window channels (indices 646–921), the best analysis fit is found in the OEC-based run, while the difference between the operational and reference runs is small. The difference between the OEC-based and other runs is larger in the extratropics than in the tropics and it is the largest on the cleanest window channels. This suggests that accounting for the OEC improves the analysis fit primarily by increasing the control over skin temperature.

Comparison of background fit to independent observations shows only small differences between the three runs. Background fits are shown in Fig. 6 for some conventional and space-borne microwave data. Radiosonde and aircraft temperature data (black and blue lines in the left-hand-panels) show no impact at all. There is a small positive impact on the fit to radiosonde specific humidity (red lines) in the upper troposphere in both the reference (top panels) and OEC-based (bottom panels) runs. In the OEC-based run only, the positive humidity impact extends to mid- and lower troposphere. Microwave radiance data (right-hand-panels) shows more improvement in the OEC-based run than in the reference run, especially on stratospheric-peaking channels of AMSU-A and ATMS. However, these impacts are very small.

Headline forecast scores for the reference and OEC-based runs are shown in Fig. 7. The scores are normalized by the operational run. In both runs, there is a positive (but non-significant) impact on 500 hPa geopotential forecasts in the Northern extratropics (left panels), while the impact in the Southern extratropics (middle panels) is smaller. The largest impact is found on 200 hPa geopotential in Tropics (right panels), where the positive impact is statistically significant up to the range of four days in the reference run and six days in the OEC-based run. In general, the OEC-based run shows marginally improved forecast scores as compared with the reference run.

5.3 Summary of the performance evaluation

In the theoretical comparison, the OEC-based channel list outperforms the reference and operational lists in the analysis of both upper- and lower-tropospheric humidity and mid-tropospheric temperature. When it comes to practical assimilation experiments, there are little indications of improved performance. Consistently with the theoretical result, humidity-sensitive background departure data show a small positive

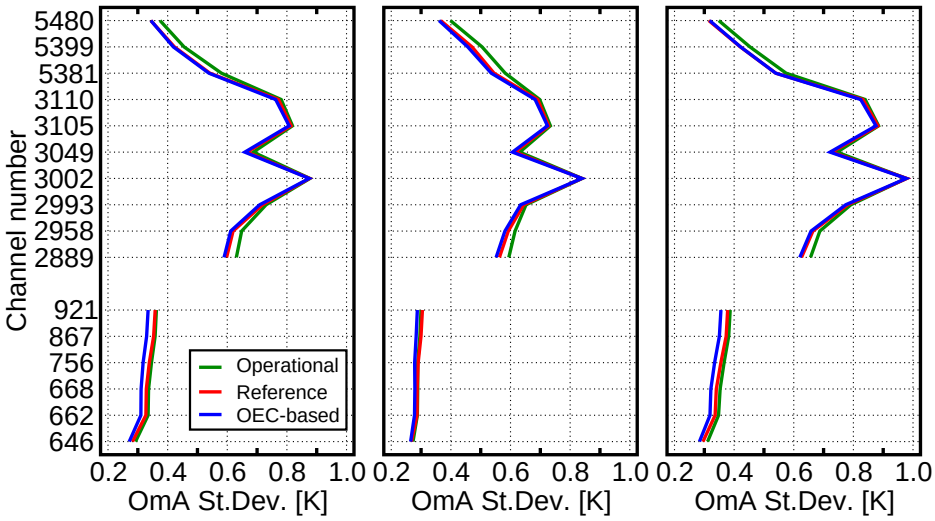

Fig. 5: Standard deviation of Observation minus Analysis (OmA) departure in the Northern extratropics (left), Tropics (middle), and Southern extratropics (right) in data assimilation experiments using either the operational IASI channel list (green), reference list (red) or OEC-based list (blue).

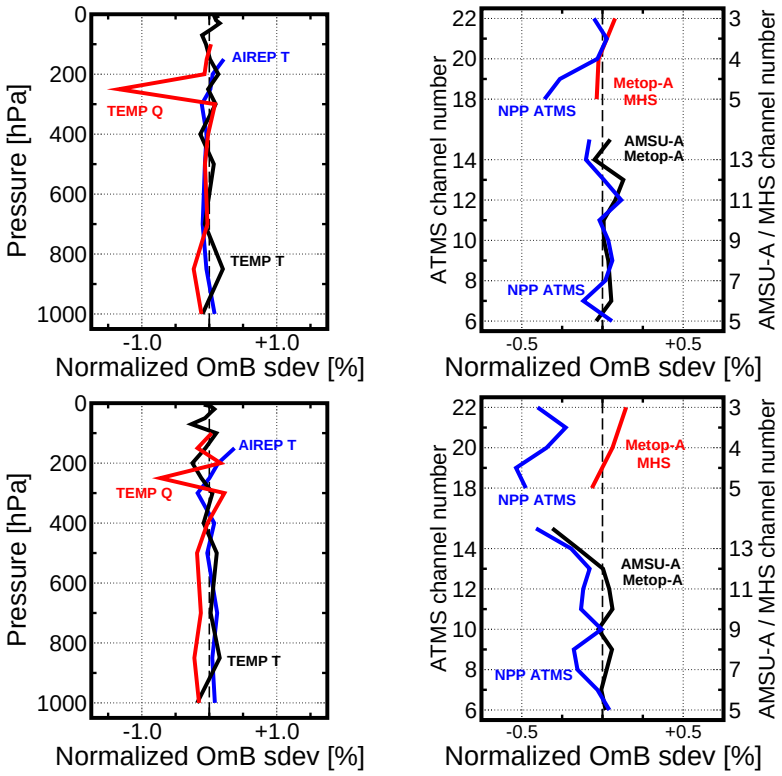

Fig. 6: Normalized global background departure standard deviations for some conventional (left) and space-borne microwave radiance (right) observations in the reference (top) and OEC-based (bottom) runs. Normalization is with respect to the operational run, and negative values imply improved background fit.

impact in the OEC-based run, but no similar impact can be identified on data that is sensitive to temperature in the mid-troposphere. Although the OEC-based run shows performance that is generally similar to that of reference and operational runs, even better evaluation scores could be expected on the basis of the theoretical comparison.

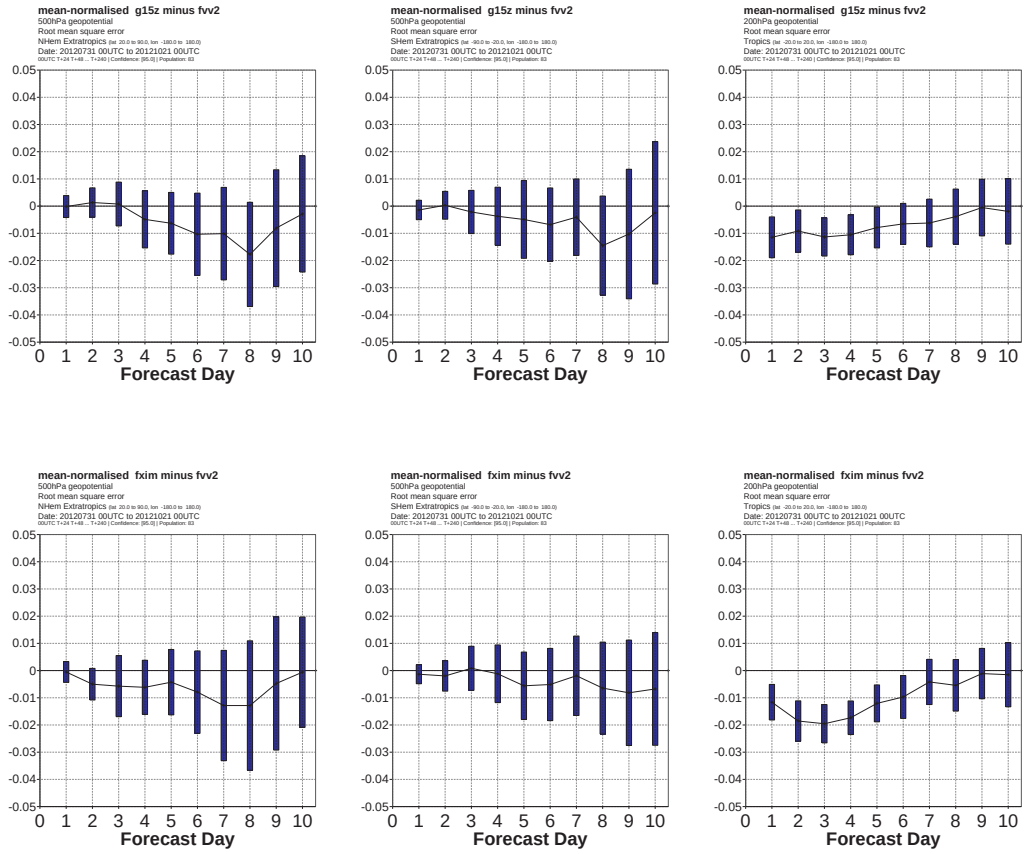

Fig. 7: Control-normalized root-mean-squared error in geopotential forecast at 500 hPa in the Northern (left) and Southern (middle) extratropics and at 200 hPa in the Tropics (right) as a function of forecast lead time. Scores are shown for the reference run (top panels) and for the OEC-based run (bottom panels). Normalization is with respect to the operational run and negative values imply improved forecast system performance. Bars indicate the 95% confidence intervals.

The theoretical performance gain of the OEC-based channel list can largely be attributed to improved capability to resolve ambiguous signals that can be produced by either temperature or humidity background errors. It is unclear to which extent such ambiguities can be resolved in practical 4D-Var assimilation systems. Theoretical considerations suggest that channels hitting water vapour absorption lines in the long-wave window region could provide useful information for lower-tropospheric humidity analysis, given that background and observation error covariances are correctly specified. Nevertheless, it is common practice to not assimilate these channels in operations, as past experience suggests that if given a significant weight in the analysis, they are more likely to degrade than improve the overall performance of the forecast system. Whether or not this is the case even if the OEC is properly taken into account, remains to be found out in future experiments.

The improved analysis fit to window channels (see Fig. 5) suggests that the additional information associated with the OEC is largely spent in the analysis of skin temperature. This is sub-optimal, as skin temperature is used as a sink variable and has no direct influence on forecast atmospheric variables. In order to direct the analysis increment more towards atmospheric variables and less towards the skin temperature, one could try decreasing the value specified to the skin temperature background error variance.

6 Conclusions

Using a simple illustration of linear analysis, we have demonstrated that presence of OEC allows improved retrieval of information contained in observations, as compared with the case of uncorrelated observation errors. Motivated by this theoretical result, we have investigated the role of OEC on optimization of IASI channel list used in realistic NWP applications. Two channel lists are derived, one (reference) where observation errors are assumed to be uncorrelated, and another (OEC-based) where OEC introduced by the signal apodization is explicitly taken into account. Other sources of OEC are ignored in this work. The OEC-based channel list is found to contain fewer stratospheric- and upper-tropospheric-sensitive channels and more lower-tropospheric channels, than the reference list. While both new channel lists indicate improved theoretical performance as compared with the currently-operational list of channels, the information content is the highest in the OEC-based list. The theoretical gain in information content comes from improvements in the analysis of upper- and lower-tropospheric humidity and mid-tropospheric temperature.

Despite the theoretical performance gain, there are little indications of improved forecast system performance when the operational channel list is replaced either by the reference list or OEC-based list. Observation minus analysis departure statistics suggest increased control over skin temperature analysis through accounting for the OEC in the channel selection. However, this does not translate into improved background fit when independent observations are considered. As compared with the reference list, the OEC-based list shows slightly improved background fit to radiosonde specific humidity and stratospheric-peaking AMSU-A and ATMS channels. The new channel lists have a positive forecast impact in the Northern extratropics, when compared against the operational list, but the benefit from accounting for the OEC appears very small. Further work is needed before full information content associated with OEC can be exploited in a state-of-the-art NWP system.

Acknowledgements

Reima Eresmaa has received funding for this work through the EUMETSAT NWP SAF Programme.

References

Bormann, N., A. Collard, and P. Bauer, 2009: Estimates of spatial and inter-channel observation error characteristics for current sounder radiances for NWP. ECMWF Tech. Memo. 600, 41 pp.

Collard, A., 2007: Selection of IASI channels for use in numerical weather prediction. *Q. J. R. Meteorol. Soc.*, **133**, 1977–1991.

Collard, A. and A. McNally, 2009: The assimilation of Infrared Atmospheric Sounding Interferometer radiances at ECMWF. *Q. J. R. Meteorol. Soc.*, **135**, 1044–1058.

Ventress, L. and A. Dudhia, 2014: Improving the selection of IASI channels for use in numerical weather prediction. *Q. J. R. Meteorol. Soc.*, doi:10.1002/qj.2280.

Weston, P., W. Bell, and J. Eyre, 2014: Accounting for correlated error in the assimilation of high-resolution sounder data. *Q. J. R. Meteorol. Soc.*, doi:10.1002/qj.2306.